3 Surfaces and Interfaces

3-1 Structure and Initial Oxidation of the SiC(0001) Surface

The oxidation of semiconductors is an important topic in the context of the fabrication of electronic devices, as well as of strong interest from the viewpoint of fundamental science. Silicon carbide (SiC) is expected to play an increasing role as a material for electronic devices, such as power devices. To realize its full potential, it is necessary to improve the quality of the interface between SiC and silicon oxide. A better understanding of the oxidation mechanism is essential for this purpose. SiC is also very interesting for comparison with silicon. For example, surface structures that consist mainly of Si atoms can be prepared that have a different atomic and electronic structure than silicon surfaces.

In this work, we have investigated the initial oxidation of the SiC(0001)-3×3 surface at room temperature using surface X-ray diffraction. Two fundamentally different models have been proposed for the initial oxidation of this surface. In the first one the lower layers of the surface are oxidized before the very top layer [1], while in the second one the topmost Si atoms on the surface are oxidized first [2].

The experiment was carried out at BL-15B2, where a six-circle diffractometer coupled to an ultra-high vacuum chamber is installed. The sample was kept under ultra-high vacuum conditions (base pressure 3×10^{-10} Torr) during the whole experiment. The 3×3 surface reconstruction was prepared by depositing several nanometers of Si at room temperature onto the surface of a 4H-SiC (0001) sample, and then heating the sample to about 1075°C for 1 min. This resulted in a sharp 3×3 RHEED (Reflection High-Energy Electron Diffraction) pattern. The surface was then exposed to about 30 L of oxygen at room temperature.

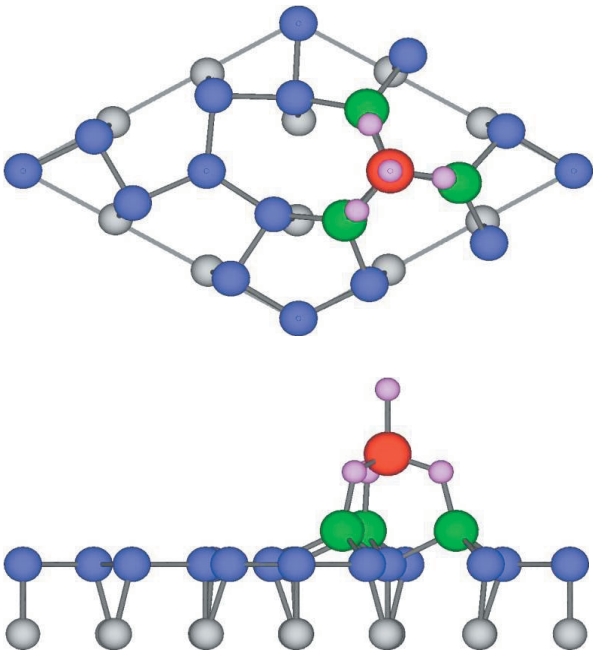

Figure 1
Structure of the oxidized SiC(0001)-3×3 surface. Oxygen atoms are shown in pink, all other atoms are silicon atoms.

The surface structure was determined before and after oxygen exposure by fitting the intensities calculated from model structures to those determined from measurements of the in-plane and out-of-plane intensities of fractional-order reflections.

The Patterson map of the diffracted intensities gives information about the inter-atomic vectors in the real-space structure. By comparing the Patterson maps of the intensities before and after oxidation, it was found that the main changes occurred at the Si tetramer on the top of the surface [3]. This compares well to the model of Xie *et al.* [2].

Different models for the oxidized structure were fitted to the experimental data. The best agreement between calculated and measured intensities was found for a model similar to that of Xie *et al.* [2], as shown in Fig. 1. Three oxygen atoms (pink) are inserted into the backbonds of the topmost Si adatom (red), with another oxygen atom on top. The positions of the atoms of the Si adlayer below (blue) are mostly unaffected [3]. In Fig. 2 the experimental structure factors and those calculated from the best-fit model are shown.

It is interesting to compare this structure with that found after the initial oxidation of the SiC(0001)-√3×√3 surface [4] and the Si(111)-7×7 surface. The local structure near the oxidized adatom in these structures is very similar to that in the SiC(0001)-3×3 surface.

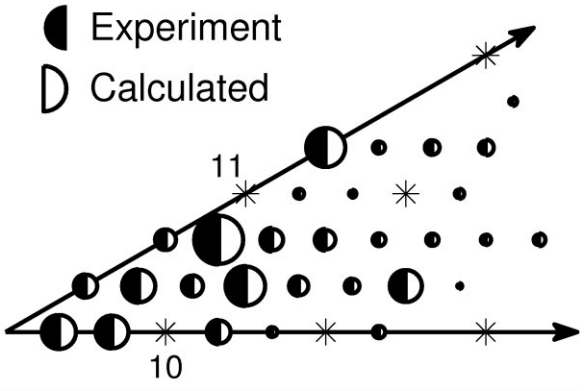

Figure 2
Structure factors from experiment (black) and calculated from the best-fit model (white).

W. Voegeli[1], K. Akimoto[1], T. Urata[1], S. Nakatani[2], K. Sumitani[2], T. Takahashi[2], Y. Hisada[3], Y. Mitsuoka[3], S. Mukainakano[3], H. Sugiyama[4], X.-W. Zhang[4] and H. Kawata[4] ([1]Nagoya Univ., [2]ISSP, the Univ. of Tokyo, [3]DENSO CORP., [4]KEK-PF)

References

[1] F. Amy, H. Enriquez, P. Soukiassian, P.-F. Storino, Y.J. Chabal, A.J. Mayne, G. Dujardin, Y.K. Hwu and C. Brylinski, *Phys. Rev. Lett.*, **86** (2001) 4342.

[2] X. Xie, K.P. Loh, N. Yakolev, S.W. Yang and P. Wu, *J. Chem. Phys.*, **119** (2003) 4905.

[3] W. Voegeli, K. Akimoto, T. Urata, S. Nakatani, K. Sumitani, T. Takahashi, Y. Hisada, Y. Mitsuoka, S. Mukainakano, H. sugiyama, X.-W. Zhang and H. Kawata, *Surf. Sci.*, **601** (2007) 1048.

[4] W. Voegeli *et al.*, in preparation.

3-2 A Resonant Photoemission Study of $SrTiO_3/LaTiO_3$ Interfaces

Following recent developments in oxide thin film fabrication techniques, atomically controlled heterostructures of transition-metal oxides have become available, and are attracting considerable attention. Ohtomo *et al.* [1] made an atomic-resolution electron-energy-loss spectroscopy study of one to two layers of the Mott insulator $LaTiO_3$ (LTO) embedded in the band insulator $SrTiO_3$ (STO), and found that the Ti *3d* electrons are not completely confined within the LTO layer but are spread over the neighboring STO layers in spite of the chemically abrupt interfaces. Okamoto and Millis [2, 3] studied the spectral function of such systems using a model Hartree-Fock and dynamical-mean-field-theory (DMFT) calculation and predicted a novel metallic behavior at the interface between the two insulators.

To gain further insight into the electronic structure of the interfaces, information on the electronic density of states near the Fermi level (E_F) is essential. Photoemission spectroscopy (PES) is an ideal tool to obtain such information, but the short mean-free path of photoelectron has generally prohibited access to the interfacial region buried in the sample. In this work we have used giant resonant PES (Ti $2p \rightarrow 3d$) to study STO/LTO superlattices.

The STO/LTO superlattice films were grown on 0.05 wt% Nb-doped STO (001)-oriented single-crystal substrates using the pulsed laser deposition (PLD) technique. Details of the fabrication and characterization of the films are described elsewhere [4], and schematic views of the fabricated thin films are shown in Fig. 3.

The resonant PES measurements were performed at BL-2C using a Scienta SES-100 analyzer with the total energy resolution set to about 150 meV. Samples were transferred from the PLD chamber to the spectrometer chamber through air, and no surface treatment was made prior to the resonant PES measurements,

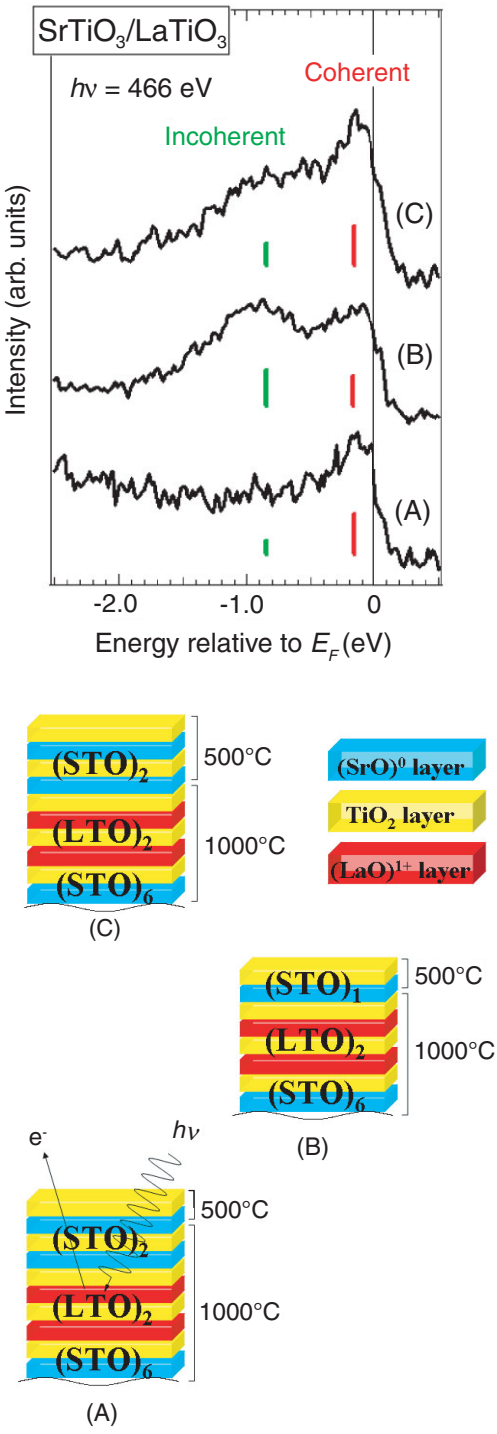

Figure 3
Ti $2p \rightarrow 3d$ resonant PES spectra of the $SrTiO_3/LaTiO_3$ superlattice samples recorded at a photon energy of 466 eV. Schematic views of the superlattice samples:-(A), the "2 unit cell capped and annealed" sample, (B), the "1 unit cell capped" sample, and (C), the "2 unit cell capped" sample. The growth temperatures are also indicated.

which were all made at room temperature.

Figure 4 shows typical resonant PES spectra recorded at various photon energies, together with the corresponding X-ray absorption spectra. The spectra of STO showed a wide gap of about 3 eV, consistent with the optical band gap. Emission within the gap was strongly enhanced at the energies of absorption maxima, and these structures can therefore be unambiguously attributed to Ti *3d* states.

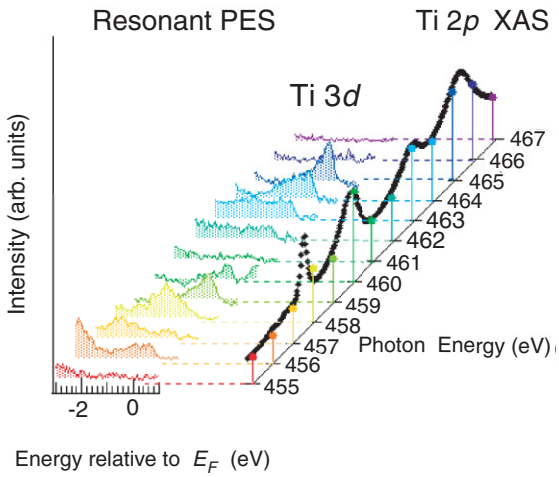

Figure 4
Ti 2*p* X-ray absorption spectrum (XAS) and resonant PES spectra of sample (A) (see Fig. 3).

The upper panel of Fig. 3 shows the Ti 3*d* states observed in the resonant PES spectra at 466 eV for the STO/LTO superlattices. A Fermi cut-off appears for all three samples, an observation which may be consistent with "electronic reconstruction" at the interface between the Mott insulator and the band insulator [2, 3]. Spectral changes are seen depending on the number of top STO layers and on the growth temperature. These spectral changes were well reproduced by DMFT calculations for heterostructure models [5].

In conclusion, we have studied the electronic structure of STO/LTO interfaces using resonant PES. We observed a metallic Fermi edge, indicating the formation of a metallic interface between the Mott insulator LTO and the band insulator STO. The spatial extent of the Ti 3*d* electrons plays an important role in explaining the different spectral features near E_F.

M. Takizawa[1], H. Wadati[1], K. Tanaka[1], M. Hashimoto[1], T. Yoshida[1], A. Fujimori[1], A. Chikamatsu[1], H. Kumigashira[1], M. Oshima[1], K. Shibuya[2], T. Mihara[3], T. Ohnishi[2], M. Lippmaa[2], M. Kawasaki[4], H. Koinuma[3], S. Okamoto[5] and A. J. Millis[5] ([1]The Univ. of Tokyo, [2]ISSP, The Univ. of Tokyo, [3]Tokyo Inst. of Tech., [4]Tohoku Univ., [5]Columbia Univ.)

References

[1] A. Ohtomo, D.A. Muller, J.L. Grazul and H.Y. Hwang, *Nature*, **419** (2002) 378.
[2] S. Okamoto and A.J. Millis, *Nature*, **428** (2004) 630.
[3] S. Okamoto and A.J. Millis, *Phys Rev. B*, **70** (2004) 241104.
[4] K. Shibuya, T. Ohnishi, M. Kawasaki, H. Koinuma and M. Lippmaa, *Jpn. J. Appl. Phys.*, **43** (2004) L1178.
[5] M. Takizawa, H. Wadati, K. Tanaka, M. Hashimoto, T. Yoshida, A. Fujimori, A. Chikamatsu, H. Kumigashira, M. Oshima, K. Shibuya, T. Mihara, T. Ohnishi, M. Lippmaa, M. Kawasaki, H. Koinuma, S. Okamoto and A.J. Millis, *Phys. Rev. Lett.*, **97** (2006) 057601.

3-3 Interface Dipole Formation at Polar/Non-Polar Heterointerfaces of Transition Metal Oxides

There has been a great deal of interest recently in spin tunnel junctions employing ferromagnetic oxides as electrodes because of their potential applications to spintronic devices, such as tunneling magnetoresistance (TMR) devices [1, 2] and ferromagnetic field-effect transistors [3]. The half-metallic ferromagnetic oxide $La_{0.6}Sr_{0.4}MnO_3$ (LSMO), which has optimal hole doping, is a promising material for use in spintronic devices owing to its half metallic nature and high Curie temperature [4]. However, the performance of TMR devices based on LSMO and $SrTiO_3$ (STO) barriers is far worse than what would be expected from the high spin polarization of LSMO, suggesting the formation of an interface layer with reduced spin polarization [1]. In contrast to the LSMO/STO interface, a robust spin polarization has been reported to exist at the $SrRuO_3$ (SRO)/STO interface [5]. Since the performance of spintronic devices is very sensitive to the interfacial electronic states, a detailed investigation of the interfacial electronic structure is crucial for designing spintronic devices based on transition metal oxides. Especially, it is important to determine the band diagrams of the Schottky junctions which dominate the performance of spintronic devices. Here, we report band diagrams determined by *in situ* photoemission (PES) measurements for Schottky junctions formed at the LSMO/Nb-doped STO (Nb:STO) and SRO/Nb:STO interfaces [6].

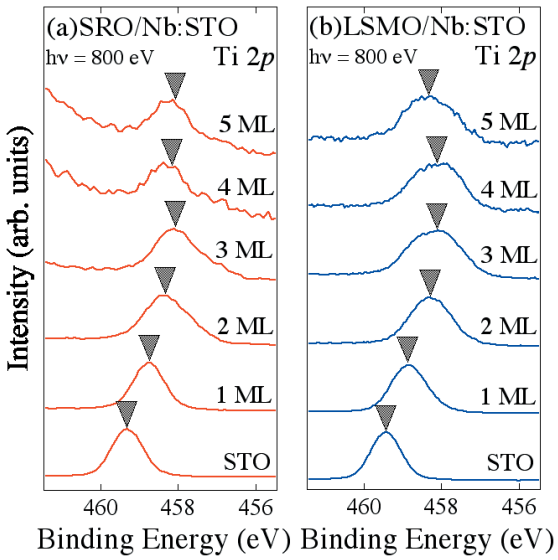

Figure 5
Ti 2*p* core-level spectra of Nb:STO buried in (a) SRO overlayers and (b) LSMO overlayers.

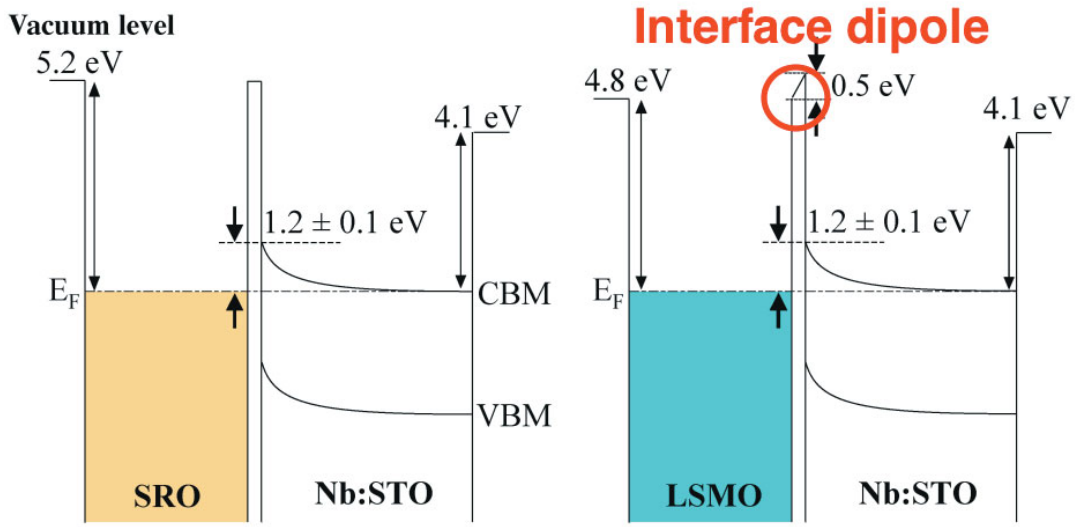

Figure 6
Band diagrams of SRO/Nb:STO (left) and LSMO/Nb:STO (right) Schottky junctions determined using *in situ* photoemission spectroscopy.

LSMO and SRO thin films were grown on TiO_2-terminated Nb:STO substrates in a laser molecular beam epitaxy (laser MBE) chamber connected to the synchrotron-radiation photoemission system at BL-2C. Figure 5 shows the Ti 2*p* core-level spectra of the buried Nb:STO for both junctions. Study of these spectra enables us to determine the barrier heights of the heterojunctions directly. Judging from the energy shifts of the core-level peak positions, the Schottky barrier heights (SBHs) for both junctions can be estimated to be 1.2 ± 0.1 eV. On the other hand, the work functions of the SRO film, the LSMO film, and the Nb:STO substrate were determined to be 5.2 ± 0.1, 4.8 ± 0.1, and 4.1 ± 0.1 eV respectively by determining the onsets of secondary electron emission.

The band diagrams for SRO/Nb:STO and LSMO/Nb:STO as determined from the present PES experiments are illustrated in Fig. 6. Assuming that ideal Schottky barriers are formed at the interfaces (Schottky limit), the SBH at the SRO/Nb:STO heterointerface should be 1.1 ± 0.1 eV, and that at the LSMO/Nb:STO heterointerface 0.7 ± 0.1 eV. The excellent agreement between the observed SBH and the prediction from the Schottky-Mott rule for the SRO/Nb:STO indicates that an ideal Schottky barrier is indeed formed at the SRO/Nb:STO heterointerface. By contrast, the measured SBH of LSMO/Nb:STO is larger by 0.5 eV than the predicted value, suggesting the formation of an interface dipole [6].

Although the origin of this interface dipole is not yet clear, there are two possible explanations: a polarity discontinuity [7] at the interface between polar LSMO ($MnO_2^{0.6-}$ / $La_{0.6}Sr_{0.4}O^{0.6+}$ / $MnO_2^{0.6-}$ / …) and nonpolar STO, or the rearrangement or replacement of constituent atoms induced by lattice mismatch [8] between films and substrates at the heterointerface. In order to identify the origin of interface dipole formation at metallic oxide/Nb:STO Schottky junctions, further systematic investigation is necessary. It is especially important to clarify how the terminating layers of substrates affect the formation of Schottky barriers and interface dipoles.

M. Minohara, I. Ohkubo, H. Kumigashira and M. Oshima (The Univ. of Tokyo)

References

[1] H. Yamada, Y. Ogawa, Y. Ishii, H. Sato, M. Kawasaki, H. Akoh and Y. Tokura, *Science*, **305** (2004) 646.
[2] T. Obata, T. Manako, Y. Shimakawa and Y. Kubo, *Appl. Phys. Lett.*, **74** (1999) 290.
[3] T. Kanki, Y.G. Park, H. Tanaka and T. Kawai, *Appl. Phys. Lett.*, **83** (2003) 4860.
[4] J.H. Park, E. Vescovo, H.J. Kim, C. Kwon, R. Ramesh and T. Venkatesan, *Nature*, **392** (1998) 794.
[5] K.S. Takahashi, A. Sawa, Y. Ishii, H. Akoh, M. Kawasaki and Y. Tokura, *Phys. Rev. B,* **67** (2003) 094413.
[6] M. Minohara, I. Ohkubo, H. Kumigashira and M. Oshima, *Appl. Phys. Lett.*, **90** (2007) 132123.
[7] N. Nakagawa, H.Y. Hwang and D.A. Muller, *Nature Mater.*, **5** (2006) 204.
[8] F. Bernardini and V. Fiorentini, *Phys. Rev. B,* **57** (1998) R9427.